A Numerical Study of the Composite Surface Model for Ocean Backscattering

Joel T. Johnson, *Member, IEEE,* Robert T. Shin, *Senior Member, IEEE,* Jin Au Kong, *Fellow, IEEE,* Leung Tsang, *Fellow IEEE,* and Kyung Pak

***Abstract*— A numerical study of 14-GHz backscattering from ocean-like surfaces, described by a Pierson–Moskowitz spectrum, is presented. Surfaces rough in one and two dimensions are investigated, with Monte Carlo simulations performed efficiently through the use of the canonical-grid expansion in an iterative method of moments. Backscattering cross sections are illustrated for perfectly conducting surfaces at angles from 0 to 60° from normal incidence, and the efficiency of the numerical model enables the composite surface theory to be studied in the microwave frequency range for realistic one-dimensional (1-D) surface profiles at low wind speeds (3 m/s). Variations with surface spectrum low-frequency cutoff (ranging over spatial lengths from 21.9 to 4.29 cm) are investigated to obtain an assessment of composite surface model accuracy. The 1-D surface results show an increase in hh backscatter returns as surface low-frequency content is increased for incidence angles larger than 30°, while vv returns remain relatively constant, all as predicted by the composite surface model. Similar results are obtained for surfaces rough in two dimensions, although the increased computational complexity allows maximum surface sizes of only 1.37 m to be considered. In addition, cross-polarized cross sections are studied in the two-dimensional (2-D) surface case and again found to increase as surface low-frequency content is increased. For both 1-D and 2-D surfaces, backscattering cross sections within 20° of normal incidence are found to be well matched by both Monte Carlo and analytical physical optics (PO) methods for all low-frequency cutoffs considered, and a comparison of analytical PO and geometrical optics (GO) results indicates an appropriate choice of the cutoff wavenumber in the composite surface model to insure an accurate slope variance for use in GO predictions. This choice of cutoff wavenumber is then applied in the composite surface theory for more realistic ocean spectra and compared with available experimental data.**

Manuscript received February 26, 1996; revised January 22, 1997. This work was sponsored by ONR Contract N00014-92-J-1616, NASA Contract 958461, and a National Science Foundation graduate fellowship. Use of the IBM SP/2 at the Maui High Performance Computing Center is acknowledged, sponsored by the Phillips Laboratory, Air Force Material Command under Cooperative Agreement F29601-93-2-0001. Opinions, interpretations, conclusions, and recommendations are those of the authors and are not necessarily endorsed by the United States Air Force, Phillips Laboratory, or the U.S. Government.

J. T. Johnson is with the Department of Electrical Engineering and the ElectroScience Laboratory, The Ohio State University, Columbus, OH 43210 USA (e-mail: johnson@ee.eng.ohio-state.edu).

R. T. Shin and J. A. Kong are with the Department of Electrical Engineering and Research Laboratory of Electronics, Massachusetts Institute of Technology, Cambridge, MA 02139 USA.

L. Tsang is with the Electromagnetics and Remote Sensing Laboratory, Department of Electrical Engineering, University of Washington, Seattle, WA 98195-2500 USA (e-mail: tsang1@ee.washington.edu).

K. Pak is with the Radar Science and Engineering Section, Jet Propulsion Laboratory, California Institute of Technology, Pasadena, CA 91109 USA.

Publisher Item Identifier S 0196-2892(98)00140-5.

I. Introduction

SCATTERING from the ocean surface has been of interest since the development and application of radar in maritime environments in the 1940's [1]. Theories for the prediction of ocean backscatter have been developed primarily through application of the standard physical optics (or "Kirchhoff Approach") [2] or small perturbation method (SPM) [3] analytical approaches to scattering from a randomly rough surface, with a combination of these two techniques resulting in the widely-used composite surface (or "two scale") model [4]–[6] of ocean backscatter. Additional analytical theories for rough surface scattering have been developed recently [7]–[13], but have yet to obtain the popularity of the composite model. The composite surface model is based on the observation that the ocean surface contains many spatial scales, ranging from long gravity type ocean waves that can have wavelengths of hundreds of meters to short capillary type ocean waves which can have wavelengths in the millimeter range. The composite surface model states that scattering from such a surface can be calculated by dividing the surface spectrum into a "long" wavelength portion, for which the physical optics (PO) or geometrical optics (GO) approximation is applied, and a "short" wavelength portion, for which the SPM method is used. SPM predictions however are averaged over the slope distribution of the long waves to model the long wave tilting effect on the short wave portion of the spectrum.

Although the composite surface model has been successful in producing a qualitative agreement with most available ocean scattering data, its basis remains a heuristic one, as the division of the ocean surface into a "small" and "long" scale remains an unclear process. While some requirements can be made based on the limitations of the underlying approximate theories, selection of the dividing point between these two scales, known as the "cutoff" wavenumber K_d in the ocean spectrum, remains primarily a parametric fit to observed data. In addition, the PO (or GO) and SPM analytical methods which form the basis of the composite surface theory are approximate solutions to the electromagnetic boundary value problem and therefore are not accurate in general for a given surface profile. Obtaining a clear assessment of composite surface model accuracy requires comparison with a more exact solution of the boundary value problem, such as that obtained by a numerical method. Such a comparison also eliminates many of the uncertainties associated with a direct comparison of composite surface model predictions with experimental data, given the difficulties in obtaining a precise model for the ocean surface at the time and location of scattering measurements.

Numerical models have been applied extensively in the past to the rough surface scattering problem, primarily using a surface integral based method of moments since discretization is required only along the surface profile instead of throughout all of space [14]–[30]. However, the rapid increase in moment method computational complexity with number of unknowns has limited the majority of previous numerical studies to relatively short surfaces rough in one direction only. Such simulations have previously been applied to assess the composite surface theory [18]–[24] primarily in the HF-frequency range, but the small surface sizes involved in terms of an electromagnetic wavelength prevent a realistic range of ocean length scales from being included simultaneously in the microwave frequency range, where even meter scale ocean features can span many electromagnetic wavelengths. Near grazing incidence backscattering from large (500λ) ocean-like 1-D surfaces at 10 GHz was studied in [25] with the "beam simulation method," but all ocean scales were again not included simultaneously in an exact simulation. No numerical assessment for ocean-like surfaces rough in two directions has yet been obtained due to the computational intensity of numerical simulations for two-dimensional (2-D) surfaces. Numerical simulations of electromagnetic scattering from 2-D ocean-like surfaces have been performed using the approximate operator expansion technique [31], [32], but the method is limited to surfaces with small slopes.

Recently, a more efficient version of the method of moments for rough surface scattering problems which allows exact simulations for large one-dimensional (1-D) and 2-D surfaces has been developed through use of a canonical grid expansion in an iterative method of moments [27]–[30]. The method is applied in this paper in a Monte Carlo study of backscattering from large 1-D and 2-D perfectly conducting random surfaces, described as Gaussian stochastic processes with a Pierson–Moskowitz spectrum as in [21]. Comparisons are made with predictions of the SPM, both analytically evaluated and Monte Carlo simulations of PO predictions, and predictions of the composite surface model. In particular, variations in backscattered cross sections with surface low-frequency content are investigated to determine the "long" wave spectral portion's influence on overall surface cross sections. Detailed comparisons of the composite and numerical models allow an appropriate choice of the composite model "cutoff" wavenumber to be determined for further use. This choice is then applied with the composite model and a more realistic ocean spectrum to compare with available backscattering experimental data from the literature.

The next section provides an overview of the ocean surface models to be applied in this paper and a brief review of approximate theories for ocean scattering. A brief description of the numerical scattering model is given in Section III, and numerical results for 1-D and 2-D surfaces are presented in Sections IV and V, respectively. Section VI considers the composite surface model for more realistic ocean spectra.

II. Ocean Surface and Approximate Models

Surfaces to be used in the Monte Carlo simulation are modeled as realizations of a zero-mean Gaussian stochastic process. The spectrum chosen for the ocean surface is a Pierson–Moskowitz spectrum, as in [21]

$$\Psi(k,\phi) = \frac{\alpha}{4\pi k^4}\ \exp\left[-\left(\frac{\beta g^2}{k^2U^4}\right)\right] \tag{1}$$

where Ψ represents the ocean spectrum amplitude in m^4, k represents the spatial wavenumber of the ocean in radians per minute, ϕ represents the azimuthal angle of the 2-D spectrum, $\alpha = 0.008, \beta = 0.74, and g = 9.81\text{m/s}^2$, and U is the wind speed in meters per second at a height of 19.5 m. Surface spectra used in the numerical simulations however will be set to zero outside of wavenumbers $k_{dl} < k < k_{du}$ so that the effects of changing surface spectral content can be investigated. Note that the Pierson–Moskowitz spectrum does not include surface tension effects or recently proposed improved models for the capillary wave portion of the spectrum [33], but numerical and analytical model results will still be compared for exactly the same surfaces, allowing meaningful conclusions to be drawn regarding composite model accuracy. Expressions for surface height and slope variances can be found in [21]. Surface spectra for 1-D surfaces are given by $\pi|k|\Psi(|k|,0)$ as in [21], with k defined to range over both positive and negative values, and again are truncated outside of $k_{dl} < |k| < k_{du}$.

Numerically predicted backscattering cross sections will be compared with those of physical optics (PO) (both analytically and Monte Carlo ensemble averaged), geometrical optics (GO), small perturbation theory (SPM), and composite surface theory, all for exactly the same truncated Pierson–Moskowitz spectrum as used in the numerical simulations. Comparison of Monte Carlo PO results with their analytically evaluated counterparts will provide a useful tool for assessing the influence of finite surface size and finite number of realizations these on Monte Carlo predictions, as demonstrated in [17]. Expressions for 1-D surface analytical theories are available from [16] and [21], with 2-D PO [13], GO [13], SPM [34], and composite surface [6] formulations available from the literature as well. Composite surface model references from the literature [36] suggest choice of the cutoff wavenumber as approximately $k/3$ where k is the electromagnetic wavenumber, corresponding to a three-wavelength spatial scale cutoff. Numerical simulations have also been performed for small 1-D surfaces [20] which indicate that backscattering errors can be minimized for a range of incidence angles by choosing K_d as $k/2$. Appropriate choices for K_d which provide minimum error when compared to numerical simulations performed will be considered in the following sections.

III. Numerical Model for Ocean Scattering

Inclusion of all ocean scales in a numerical simulation at microwave frequencies is very difficult, given the small electromagnetic wavelength and the computational costs associated with large surface scattering problems. For example, a 3-m/s wind speed produces a Pierson–Moskowitz spectral peak at a spatial scale of 8.2 m, or 383λ at 14 GHz. Since a method of moments code will require sampling at approximately eight points per electromagnetic wavelength, a total of 3065 points are required simply to resolve this scale for 1-D surfaces. Even

larger surface sizes are required to allow use of a "tapered" beam incident field to eliminate surface edge effects while still illuminating a reasonably sized portion of the surface. A surface size of 1024λ (21.9 m) at 14 GHz was thus chosen for the 1-D simulations, resulting in 8192 points in the numerical solution. Such a large number of points would be prohibitive in previous studies, but use of the canonical grid method makes these simulations possible. Although a 3-m/s wind speed is very low in terms of typical sea states encountered, even the relatively small 4.86-cm rms height of the full Pierson–Moskowitz spectrum produces a large $k\sigma$ product of 14.25 due to the small electromagnetic wavelength. Higher wind speeds would require larger surface sizes to resolve the larger ocean length scales produced and thus become more prohibitive even for the canonical grid method. Note that the primary quantity of interest in this study is the variation in backscattering cross sections caused by changing low-frequency content of the spectrum, determined by k_{dl}. Such variations illustrate the physical processes at work in ocean scattering, at least as described by the composite surface model. Since varying the low and high frequency cutoffs of the spectrum does not affect the Bragg spectral component (unless it is directly cutoff) but does affect the slope variance of the entire spectrum simulated, these variations should illustrate any tilting effects due the "long" wavelength portion of the spectrum simulated.

Modeling the complete surface spectrum even at 3-m/s wind speed is not possible for 2-D surfaces, given the requirement of sampling in two dimensions with two unknown functions needed to model vector surface currents. The 2-D surfaces to be studied will be limited to $64\lambda \times 64\lambda$, with this relatively small surface size resulting in 524 288 unknowns in the numerical simulation. This number of unknowns remains possible with the canonical grid method, although the increased computational complexity results in fewer realizations in the Monte Carlo simulation for the 2-D case. Note that 1-D surface models do not yield predictions for cross-polarized backscattering, given the complete decoupling of h and v polarizations in the 1-D problem, so only 2-D model results will be able to provide information on cross-polarized cross section behavior.

As mentioned previously, a tapered Gaussian beam incident field is used to eliminate edge effects in the study and has the effect of reducing the angular resolution of obtained cross sections as discussed in [25]. The large 1024λ surface size used in the 1-D case allows a large Gaussian beam width of 256λ to be used, and the loss in angular resolution for incidence angles between 0 and 60° is less than $\pm 0.2°$ for all angles. In the 2-D surface case, however, a Gaussian beam width (as described in [30]) of only 16λ is possible given the 64λ surface size, causing a loss in angular resolution of $\pm 2.4°$ at 60° incidence. Although this is not a significant loss for co-polarized cross sections, cross-polarized results in the plane of incidence could potentially be affected the influence of larger cross-polarized cross sections outside the plane of incidence. Studies with the analytical models, however, show that a 64λ surface size is sufficient to reduce these contributions below observable levels.

The numerical model applied models the ocean surface as being perfectly conducting. Sea water actually is a fairly high loss medium, with a dielectric constant of approximately (39.7,40.2) at K_u band [37] which increases with decreasing frequency primarily due to ionic conductivity. However, in active remote sensing, the finite conductivity of the ocean surface is expected to have only a fairly small influence on ocean cross sections, especially when considered on a decibel scale. Given the much greater complexity associated with a penetrable surface numerical model and the fact that only perfectly conducting surface models will be compared in this paper, use of a perfectly conducting surface for the ocean should not significantly influence the results of this study. Comparisons with experimental data made in Section VI will include the effect of surface conductivity through the composite surface model.

A. Definition of Radar Cross Section

Numerical results will be presented in terms of the normalized backscattering radar cross section $\sigma_{\alpha\beta}$ in the plane of incidence, defined in terms of the ensemble average scattered field intensity as

$$\sigma_{\alpha\beta}(\theta) = \lim_{R\to\infty} \frac{4\pi R^2 \left\langle |E^s_{\alpha\beta}|^2 \right\rangle}{A|E^{(i)}_{\beta}|^2} \tag{2}$$

in the 2-D surface case, where θ refers to the polar angle of observation, α and β refer to the transmit and receive polarizations, respectively, $|E^{(i)}_{\beta}|$ refers to the magnitude of the incident field on the surface profile, A to the area of the surface profile, and the $\langle\cdot\rangle$ notation above indicates an ensemble average over realizations of the surface stochastic process. The denominator of this expression is actually evaluated as $2\eta/\cos\theta_i$ times the total power incident upon the surface for the tapered beam, given by the integration of the normal component of the incident Poynting vector over the surface profile. A slightly different definition is used in the 1-D surface case

$$\sigma_{\alpha\beta}(\theta) = \lim_{R\to\infty} \frac{R \left\langle |E^s_{\alpha\beta}|^2 \right\rangle}{A|E^{(i)}_{\beta}|^2} \tag{3}$$

as in [17]. With the above definitions, 2-D surface cross sections integrated over all scattered angles in the upper hemisphere should yield $4\pi\cos\theta_i$ while 1-D cross sections integrated over all scattering angles in the plane of incidence should yield $\cos\theta_i$. These differing normalizations are used to be consistent with the available literature, and comparisons made with the analytical theories will be made consistently.

Scattering cross sections for randomly rough surfaces can be separated into a coherent and incoherent part, defined as

$$\sigma^{\text{inc}}_{\alpha\beta}(\theta_s,\phi_s,\theta_i,\phi_i) = \lim_{R\to\infty} \frac{4\pi R^2 \left\langle |E^s_{\alpha\beta} - \langle E^s_{\alpha\beta}\rangle|^2 \right\rangle}{A|E^{(i)}_{\beta}|^2} \tag{4}$$

and

$$\sigma^{\text{coh}}_{\alpha\beta}(\theta_s,\phi_s,\theta_i,\phi_i) = \lim_{R\to\infty} \frac{4\pi R^2 |\langle E^s_{\alpha\beta}\rangle|^2}{A|E^{(i)}_{\beta}|^2} \tag{5}$$

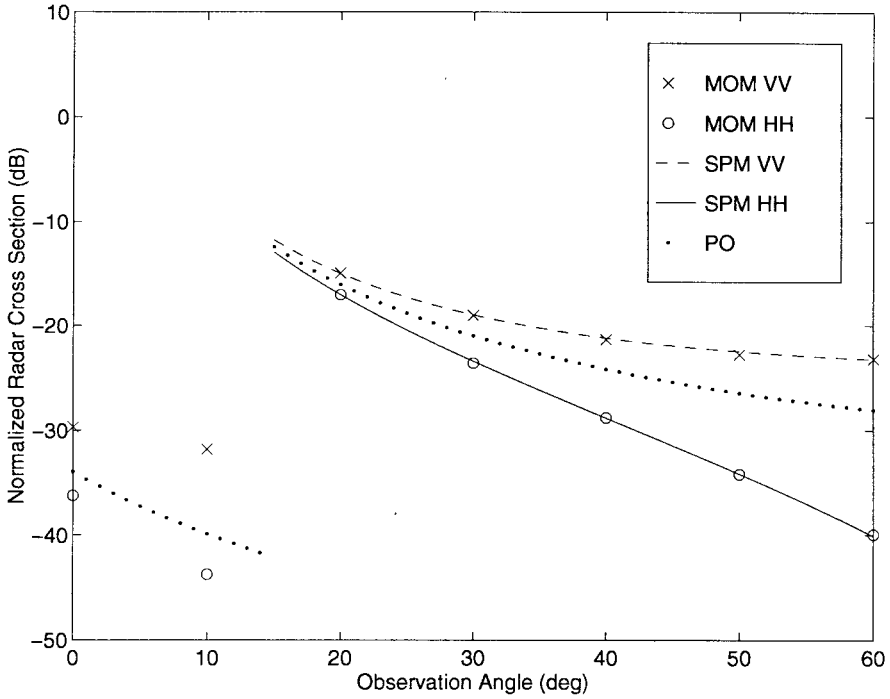

Fig. 1. A 1-D comparison of MOM, SPM, and PO backscattering predictions. Cutoff wavenumber $k_{dl} = 146.6$ rads/m, $k\sigma = 0.088$ rads/m.

in the 2-D case, with similar equations for the 1-D cross sections. For an infinitely large ocean surface, reflected and transmitted coherent fields consist of individual propagating plane waves whose amplitude is reduced as the surface height fluctuations increase. However, surfaces simulated numerically are of finite size, and the coherent field is no longer a plane wave but rather spreads over a range of scattered angles. Since scattering from the ocean is primarily incoherent at microwave frequencies, only incoherent scattered powers are of interest in the numerical simulation. In the simulation results presented in Section IV, surface rms heights ranging from 0.01–2.27 wavelengths are considered, so that coherent fields are clearly present in the lower rms height cases. The above procedure allows their influence to be removed so that only incoherent scattered powers are presented in the following results.

B. Computational Resources

Results to be presented were calculated with the IBM SP/2 400 node parallel computer at the Maui High Performance Computing Center (MHPCC) [38]. The IBM SP/2 is a collection of 400 RS-6000 (based on a POWER2 CPU) workstations, capable of around 250 MFLOP operation individually, networked through a high performance communication system to allow groups of nodes to operate in combination as a parallel processor. Software libraries are available at the center to implement interprocess communications using simple routine calls, so that development of parallel codes is relatively efficient. The codes of this paper use the parallel virtual machine (PVM) message passing library [39], which is a public domain package for UNIX communications. Due to the implicitly parallel nature of a Monte Carlo simulation, parallelization of the code was effectively perfect, with only simple process starting and monitoring routines requiring any interprocess communications.

IV. 1-D Surface Results

The 1-D surface results were generated using k_{dl} values of 146.6 (2λ), 18.3 (16λ), 2.29 (128λ), and 0.286 (1024λ) rads/m, with corresponding $k\sigma$ products of 0.088, 0.707, 5.65, and 14.25. The high frequency surface cutoff was held fixed at $k_{du} = 586(\lambda/2)$ to insure that the Bragg portion of the spectrum was adequately modeled. Strong matrix bandwidths in the canonical grid method, as described in [27]–[28], ranged from 64 points in the lowest rms height case to 512 points for the highest, with a corresponding increase in the number of canonical grid terms required from three to 15, respectively. The number of realizations averaged ranged from 640 in the lowest rms height case down to 120 in the highest, due to the increased computational requirements for the higher rms height surfaces. Computational times for a single angle, polarization, and surface realization ranged from approximately 1.5 min on a single node of the SP/2 for the low rms height cases to 24 min in the high rms height v polarization cases, illustrating the efficiency and expected rms height dependencies of the canonical grid approach.

Figs. 1 and 2 compare numerical model results with SPM and PO/GO predictions for the two extreme cases, with k_{dl} wavenumbers of 146.6 (2λ) and 0.286 rads/m $(1024\lambda$, effectively the entire Pierson–Moskowitz spectrum) respectively. SPM predictions are plotted only for angles greater than 15°, given their expected failure for near normal incidence, and the angular cutoff region in Fig. 1 due to the truncation of the surface spectrum at low frequencies is clearly evident. Note that SPM predictions in Figs. 1 and 2 are exactly the

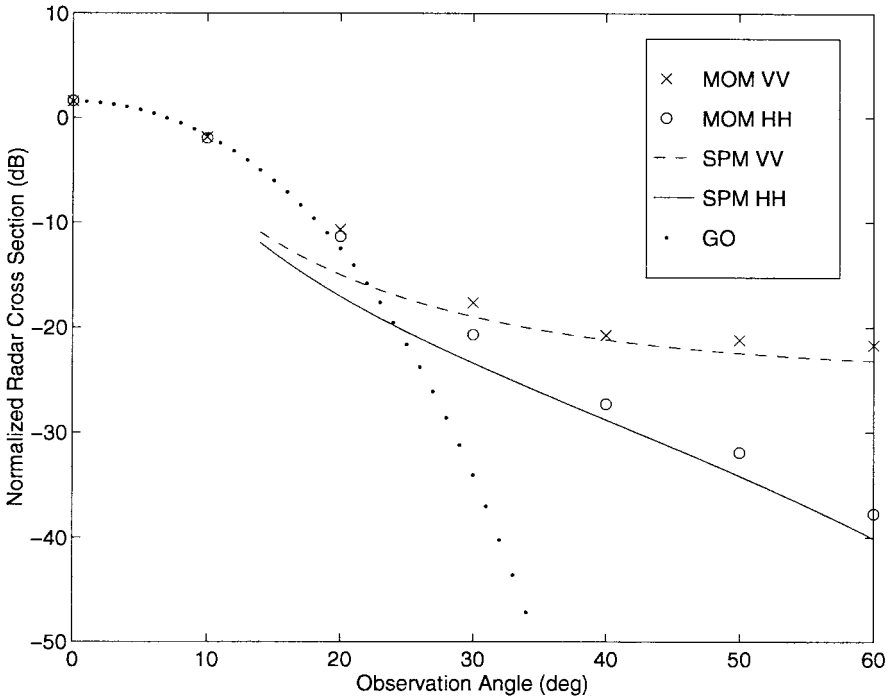

Fig. 2. A 1-D Comparison of MOM and SPM backscattering predictions. Cutoff wavenumber $k_{dl} = 0.286$ rads/m,$k\sigma = 14.25$ rads/m.

same, as Bragg scatter portions of the spectrum are not altered by changing the low-frequency cutoff. Simulation results are plotted for both hh and vv cross sections, and the excellent agreement with SPM predictions observed in the low rms height case of Fig. 1, where the SPM is expected to be very accurate, serves to validate the numerical model. PO results are observed to fall between hh and vv cross sections at large incidence angles as expected in Fig. 1, with errors in predictions for angles in the cutoff region observed as well. Fig. 2 shows that little change occurs in surface backscattering cross sections at large incidence angles as surface low-frequency content is increased dramatically, in agreement with composite surface theory. GO predictions are applied in this large $k\sigma$ product case, and are found to yield excellent predictions within 20° of normal incidence, through use of a cutoff wavenumber $K_d = k/2$ in defining the surface slope variance as discussed further in Section V. Results for the intermediate values of k_{dl} yield similar results and show a gradual transition between the curves observed in Figs. 1 and 2. In all cases, the physical optics approximation was found to fit MOM results extremely well up to 20° incidence with the exception of the errors observed in the cutoff region in Fig. 1.

Although the theoretical basis of the composite surface model is somewhat justified by numerical results, a more detailed comparison with composite surface model predictions should allow further insight into the choice of cutoff wavenumber inherent in the model. Two separate angular backscattering regions will be considered: the region between 0 and 30°, for which the physical/geometrical optics models are primarily used, and the region between 30 and 60°, for which tilted SPM predictions are primarily used. The PO/GO angular region will be considered in the next section, but Fig. 2 gives some evidence that a choice of $K_d = k/2$ should yield accurate predictions. Comparisons between method of moments results and composite surface model predictions for incidence angles between 30 and 60° are shown in Fig. 3 for the $k_{dl} = 0.286$ rads/m case, again using a cutoff wavenumber of $K_d = k/2$ to define the surface slope variance. Also included is the corresponding untilted SPM result. The change in hh cross sections is shown to agree well with the composite surface model using this value of K_d, although sensitivity to this parameter is small enough to make an thorough quantitative assessment difficult. Composite surface model results slightly underpredict numerical vv cross sections at the larger incidence angles, which will be discussed further in the next section. Overall, however, the composite surface model is qualitatively validated by these comparisons for the prediction of 0 to 60° backscattering from 1-D Pierson–Moskowitz surfaces.

V. 2-D Surface Results

The 2-D surface results were generated using k_{dl} values of 146.6 (2λ), 18.3 (16λ) and 4.58 (64λ) rads/m, with corresponding $k\sigma$ products of 0.088, 0.707, and 2.86. High frequency surface cutoff wavenumbers were again held fixed at $k_{du} = 586(\lambda/2)$ rads/m. Strong matrix bandwidths of 15 points in the canonical grid method, as described in [29]–[30], were used, with only one canonical grid series term required for these relatively low rms height surfaces, as was validated through comparisons including larger numbers of terms. The reduced bandwidth and series requirements in the canonical grid method for 2-D surfaces can be attributed to the faster decay of the Green's function in three dimensions [29]. The

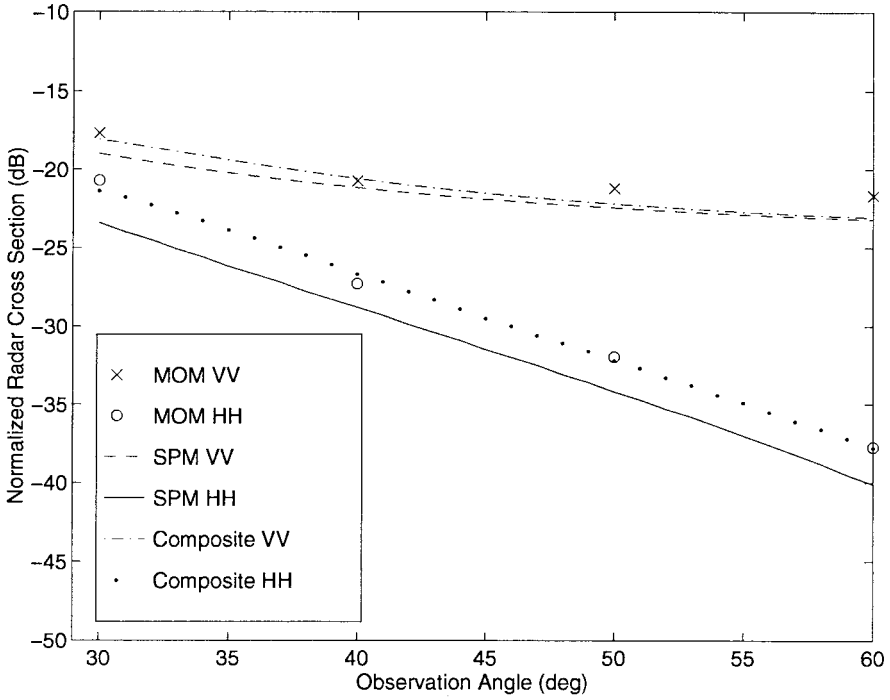

Fig. 3. A 1-D Comparison of MOM and composite surface model co-pol backscatter results.

number of realizations averaged ranged from 64 in the lowest rms height case to 128 in the highest, due to the need for more realizations of the rougher surface. Computational times for both polarizations, a single angle and surface realization ranged from approximately 4 hr on a single node of the SP/2 for the low rms height cases to 8 hr in the high rms height cases, illustrating the much greater computational complexity of the 2-D surface scattering problem. However, these computational times are very reasonable when the size of the problem (524 288 unknowns) is considered. Note that the smaller number of surface realizations averaged and the smaller tapered beam width lead to more uncertainty in 2-D results than their 1-D counterparts. However, the small rms height surfaces studied alleviate these effects somewhat, and comparisons of independent groups of 64 realizations show results to be within 1 dB accuracy. Tapered beam effects, negligible in the 1-D case, will be considered through comparison of analytically evaluated and Monte Carlo physical optics results, as discussed previously.

Figs. 4 and 5 compare 2-D numerical model results with SPM and PO/GO predictions for the two extreme cases, with k_{dl} wavenumbers of 146.6 (2λ) and 4.58 (64λ) rads/m, respectively. Simulation results are plotted for hh, hv, vh, and vv cross sections, and the model is again validated through excellent agreement with SPM predictions observed in the low rms height case of Fig. 4. Some small discrepancies are observed in Fig. 4 due to the smaller number of realizations and larger tapered beam width, but overall SPM and numerical results are within 1 dB for angles greater than 20°. Comparisons of hv and vh cross sections also show agreement to within 1 dB; note that hv and vh cross sections are not required to be equal due to tapered beam averaging over bistatic cross sections outside the plane of incidence. PO results are again observed to fall between hh and vv cross sections at large incidence angles in Fig. 4, with errors in the cutoff region again observed. These errors are not physically significant since a real ocean surface at microwave frequencies would not allow a cutoff region near normal incidence, given the large expected surface rms height in terms of a wavelength. Fig. 5 shows again that little change occurs in surface backscattering cross sections at large incidence angles as surface low-frequency content is increased dramatically. Analytical PO predictions are found to yield excellent agreement within 20° of normal incidence, with Monte Carlo PO predictions showing even better agreement with numerical results within 20°. Results for $k_{dl} = 18.3$ rads/m yield similar results, and in all cases, the physical optics approximation was found to fit MOM results extremely well up to 20° incidence with the exception of the errors observed in the cutoff region of Fig. 4.

Given the success of the physical optics approximation in matching both 1-D and 2-D numerical results up to 20°, the primary issue in the 0 to 30° region concerns the accuracy of the GO approximation, which is required for more complicated spectrum models due to difficulties associated with evaluating the full PO integral [34]. Fig. 6 compares physical/geometrical optics results for 2-D surfaces with varying values of k_{dl}, beginning with the numerically validated $k_{dl} = 4.58$ rads/m case and extending the low-frequency cutoff to include the entire 3 m/s spectrum, where 2-D simulations could not be run. A cutoff wavenumber of $K_d = k/2$ was used for the GO predictions, and is seen to produce a very good comparison with PO predictions up to approximately 15° as surface low-frequency content (and rms height) is increased. Further comparisons for higher wind speeds showed good agreement up to 20° as surface rms heights increased beyond

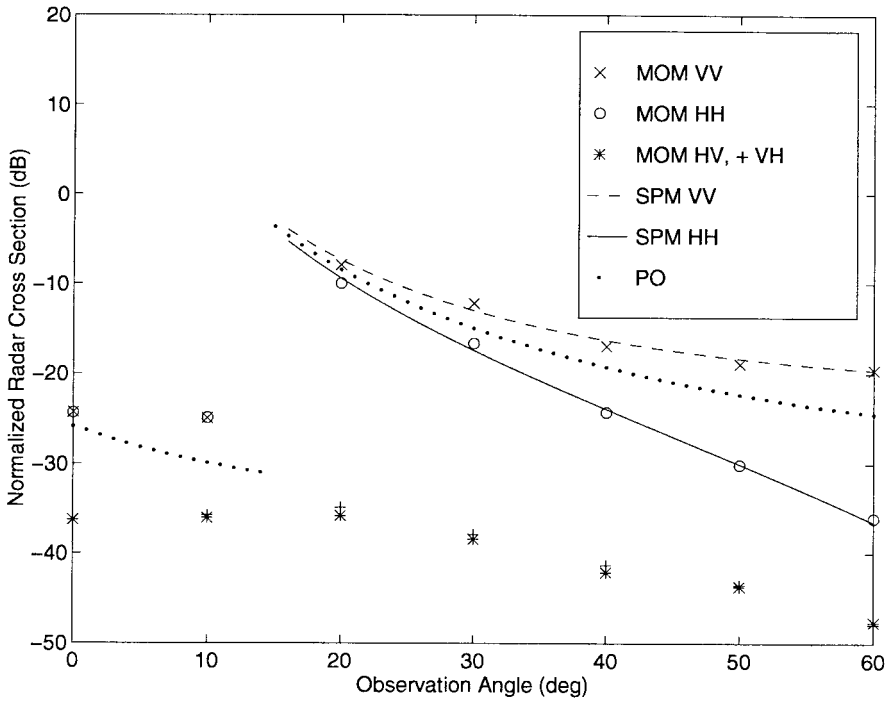

Fig. 4. A 2-D Comparison of MOM, SPM, and PO backscattering predictions. Cutoff wavenumber $k_{dl} = 146.6, k\sigma = 0.088$.

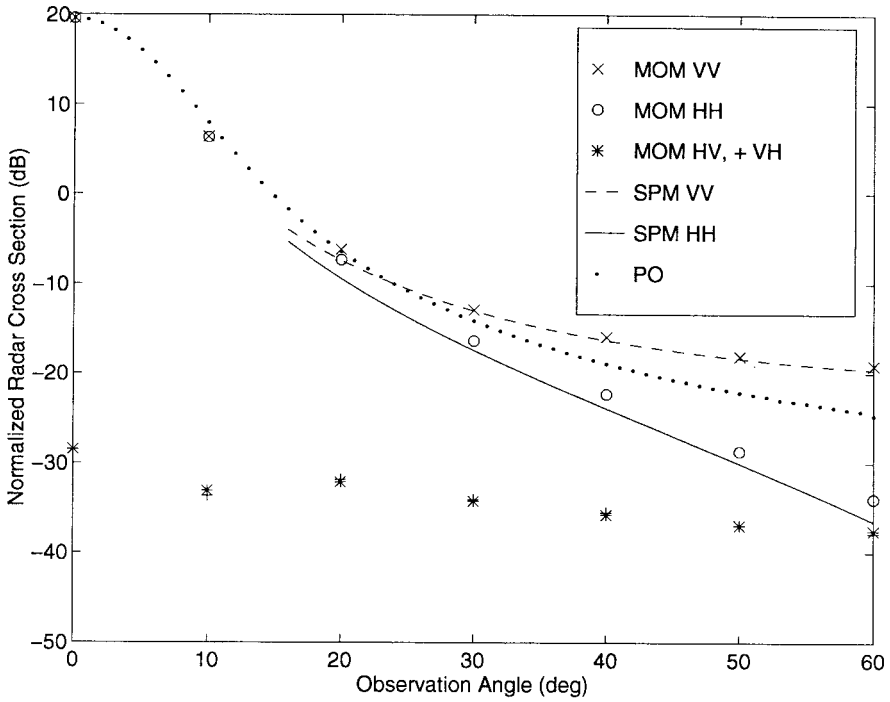

Fig. 5. A 2-D Comparison of MOM, SPM, and PO backscattering predictions. Cutoff wavenumber $k_{dl} = 4.58$ rads/m, $k\sigma = 2.86$ rads/m.

the $k\sigma = 14.25$ product obtained at 3 m/s. Alternate choices of K_d were found to produce inferior results, so a choice of $K_d = k/2$ seems optimal for backscattering predictions from a perfectly conducting Pierson–Moskowitz surface. This choice is in agreement with [20], and results in a $k\sigma$ product of 0.088 for the small scale portion of the spectrum, about one half the 0.158 value suggested by [36]. Even when including the entire slope variance of the surface, GO predictions fail to match the incidence angle dependence of PO results beyond 20° for all wind speeds considered, indicating the inherent limitations of the GO approximation in this region. However, since two scale SPM predictions produce reasonable agreement for large incidence angles, these limitations should not influence composite surface model accuracy.

Comparisons between 2-D surface results, SPM, and composite surface model predictions for incidence angles between

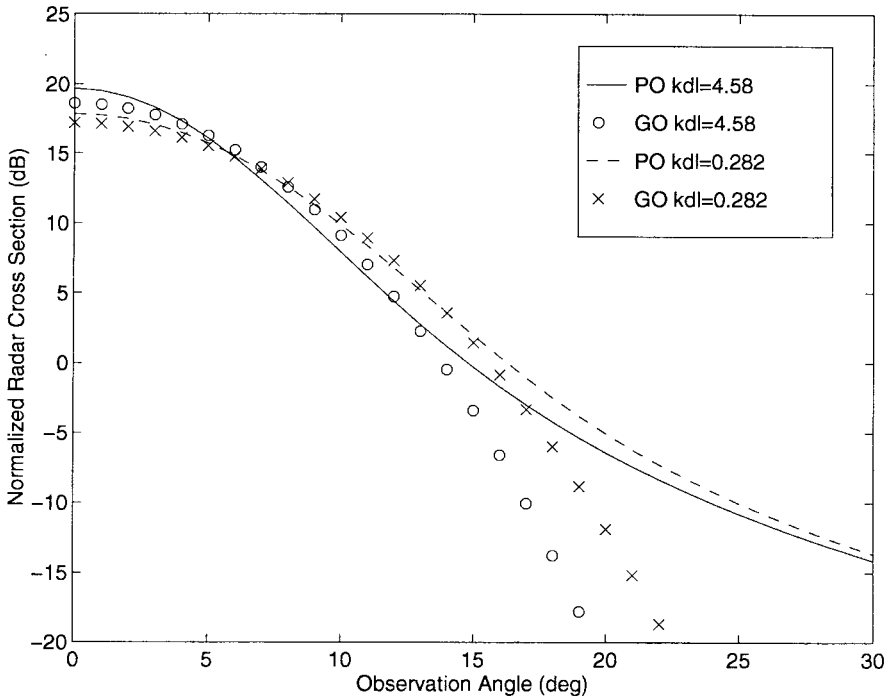

Fig. 6. Comparison of PO and GO backscattering predictions using $K_d = k/2$.

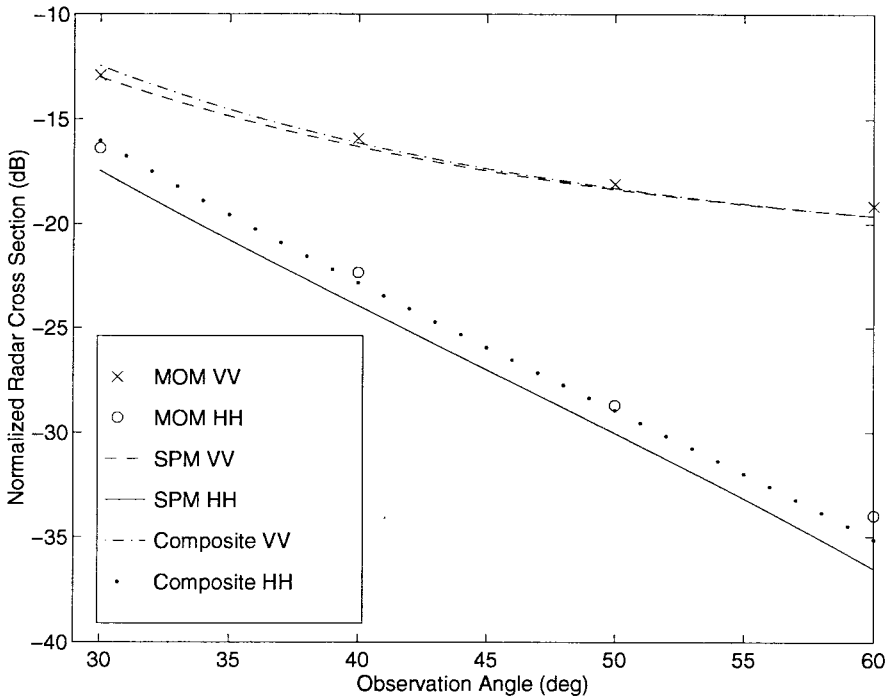

Fig. 7. A 2-D Comparison of MOM and composite surface model co-pol backscatter results.

30 and 60° are shown in Fig. 7 for the $k_{dl} = 4.58$ rads/m case, again using a cutoff wavenumber of $K_d = k/2$ to define the surface slope variance. The change in hh cross sections is shown to agree well with the composite surface model using this value of K_d, with slightly larger errors observed than in the 1-D case again due to the smaller number of surfaces averaged and the larger tapered beam width. Better agreement is observed for vv cross sections than in the 1-D case, but it should be noted that this case has a smaller total rms slope of 0.118 compared to the 0.139 rms slope of Fig. 3. Also, the effects of a given total rms slope are more pronounced in the 1-D case, since the 2-D total rms slope is split into the in-plane and out-of-plane directions. The small errors in vv cross sections observed in Fig. 3 give some indication that composite surface model vv results may be slightly inaccurate as rms slopes are increased, but a more detailed numerical study is required for further investigation. Overall, however, the composite surface model is qualitatively validated by these

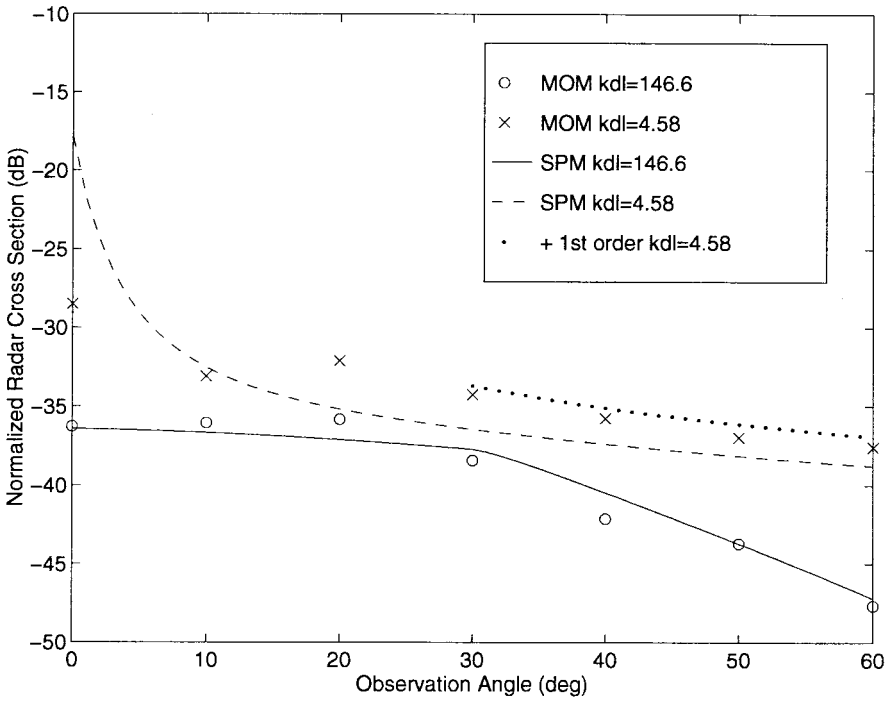

Fig. 8. Comparison of MOM and second-order cross-pol backscatter results using a conductivity of 10^{11} S/m in the SPM.

comparisons for the prediction of 0 to 60° backscattering from one and 2-D Pierson–Moskowitz surfaces.

Variations in cross-polarized cross sections with k_{dl} are plotted in Fig. 8 for the $k_{dl} = 146.6$ and 4.58 rads/m cases. Note that cross-polarized cross sections show the largest sensitivity to surface low-frequency content, with an increase of approximately 10 dB in 60° cross sections in Fig. 8. Comparison of numerical results with composite surface model predictions is complicated by the fact that second-order SPM cross-polarized cross sections are singular for a perfectly conducting surface [3], [40]. Comparisons between numerical results and second-order SPM predictions are made in Fig. 8 with a surface conductivity of 10^{11} S/m used in the SPM, chosen to set the level of SPM results near the numerical simulations. No tilting is performed for the second-order predictions, due to computational complexity of evaluating the SPM second-order cross-polarized results and the relatively flat curves for which tilting should have little effect. First-order cross-polarized cross sections, due solely to tilting effects, are also included in the $k_{dl} = 4.58$ rads/m case for incidence angles greater than 30°, where tilted SPM predictions are expected to be applicable. The comparison shows a reasonable agreement between composite surface model predictions and numerical results for incidence angles greater than 20°, where SPM predictions are expected to be valid. Note that second-order cross sections alone reproduce variations with low-frequency cutoff for cross polarization since second-order fields involve a convolution of scales within the surface spectrum rather than the single surface scale of first-order predictions. Performance for angles less than 20° is seen to be worse, as with co-polarized cross sections, indicating the inaccuracy of SPM predictions for this region. Note that geometrical optics predictions also produce no cross polarization for backscattering, and studies of Monte Carlo PO cross-polarized results near normal incidence show them to be approximately 30-dB below MOM results, indicating that the numerically obtained values are not due to beam averaging effects. These results show that near-normal incidence cross-polarized backscattering is inaccurately predicted by the composite surface model. However, given the success of the composite model in all the other regions studied, this limitation seems relatively minor.

VI. Composite Surface Model for Nonpower Law Spectra

Based on the results of the previous sections, the composite surface model should provide reasonable predictions for ocean surface backscattering given an appropriate choice of the cutoff wavenumber, at least for the Pierson–Moskowitz surfaces used in the numerical study. To consider scattering from surfaces modeled by more realistic ocean spectra, the composite surface model is applied in this section with the recently proposed Donelan–Banner–Jahne (DBJ) spectrum of [33], and results are compared with the AAFE backscatter data of [41]. A finitely conducting ocean surface is considered in this section, with a permittivity described by the model of [37].

Fig. 9 illustrates composite surface model results for backscattering using the DBJ spectrum and compares these results with the AAFE 13.9-GHz upwind data [41] at four different wind speeds. Geometrical optics and tilted SPM results are plotted separately so that individual components of the composite model can be resolved. The model is observed to produce a reasonable match to this experimental data for both polarizations over the entire range of wind speeds, although cross sections near 15° are overestimated by the GO for lower

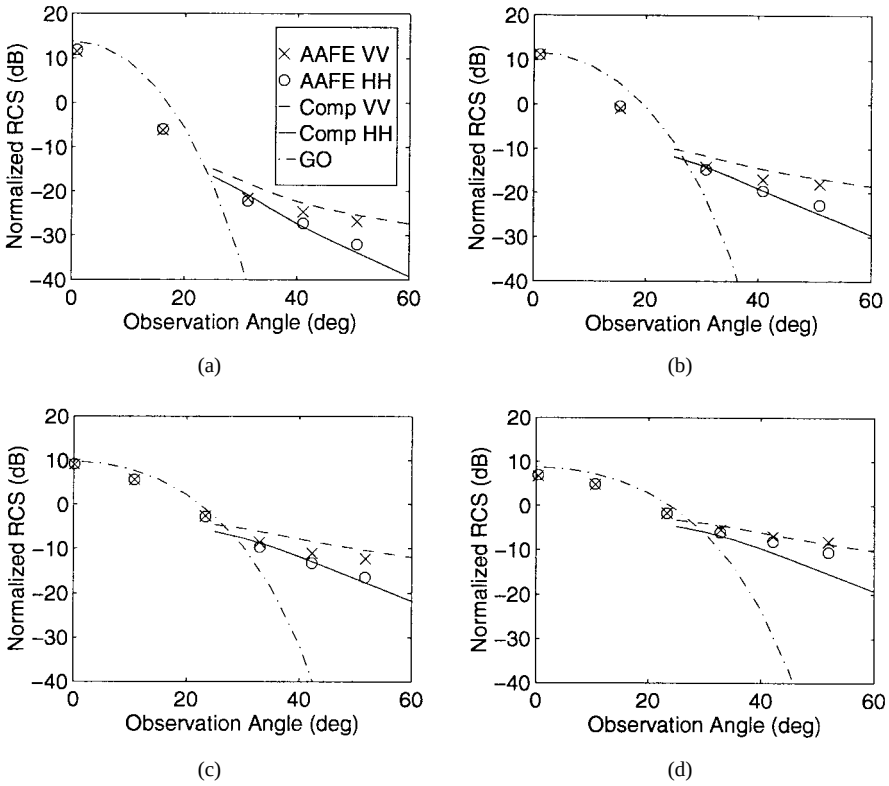

Fig. 9. Composite surface model with DBJ spectrum. Comparison with AAFE experimental backscatter data. (a) Wind speed 3.0 m/s, (b) 6.5 m/s, (c) 13.5 m/s, and (d) 23.6 m/s.

wind speeds and the greatly reduced polarization ratio at 23.6 m/s is not reproduced. Similar comparisons were made in [33] for vertical polarization, but the slope variance of the entire spectrum was used for GO predictions and found to produce inaccurate predictions near normal incidence. The good comparison obtained here gives further credence to the choice of $K_d = k/2$ obtained from the numerical model. The obtained slope variance is also seen to provide a reasonable increase in hh cross sections for incidence angles of 20° or larger at the lower wind speeds. It should be noted, however, that other ocean spectral models can be applied in the composite surface model as well to obtain similar agreement, with the minor differences which would be obtained between predictions emphasizing the importance of obtaining an accurate model for the ocean surface observed at the time and location of scattering experiments.

VII. Conclusions

A numerical model for ocean scattering has been developed and applied in a study of backscattering from a perfectly conducting 1-D and 2-D Pierson–Moskowitz surfaces. The efficiency of the canonical grid approach allowed surfaces of 1024λ in the 1-D case and $64\lambda \times 64\lambda$ in the 2-D case to be included in the numerical simulation, and backscattering simulations were performed at incidence angles up to 60° with a resulting maximum model uncertainty of approximately 1 dB. Comparisons with analytical theories show the physical optics approximation to perform well for backscattering up to 20° incidence. SPM predictions were also found to be valid for higher incidence angles as surface rms height increased beyond typical SPM limits, and slight increases in hh cross sections were also observed as predicted by the composite surface model. cross-polarized results at large incidence angles were well fit by the composite surface model as well after the inclusion of a finite surface conductivity to avoid the singularity in second-order SPM predictions for a perfectly conducting surface. Further comparisons between analytically evaluated PO and GO predictions showed an appropriate choice of cutoff wavenumber to be $K_d = k/2$ for backscattering in the composite surface model. The validated composite surface model was then used with the more realistic DBJ spectrum in a comparison with experimental data, which showed the DBJ spectrum to provide adequate predictions when appropriate tilting effects were included.

The results of this study demonstrate the importance of an accurate model for the ocean spectrum. Further research into this area continues, as there are many models in the literature which are at some variance with one another. The applicability of the composite surface model for near grazing incidence backscattering, not considered in this paper, also remains uncertain. Overall, the success of the composite surface model when compared to numerical simulations and to experimental data, however, further validates this approach for the prediction of 0 to 60° ocean scattering.

References

[1] M. I. Skolnik, *Introduction to Radar Systems*, 2nd ed. New York: McGraw-Hill, 1980.

[2] P. Beckmann and A. Spizzichino, *The Scattering of Electromagnetic Waves from Rough Surfaces*. New York: Pergamon, 1963.
[3] S. O. Rice, "Reflection of electromagnetic waves from slightly rough surfaces," *Commun. Pure Appl. Math*, vol. 4, pp. 361–378, 1951.
[4] J. W. Wright, "A new model for sea clutter," *IEEE Trans. Antennas Propagat.*, vol. AP-16, pp. 217–223, 1968.
[5] G. R. Valenzuela, "Ocean spectra for the high frequency waves as determined from airborne radar measurements," *J. Marine Res.*, vol. 29, pp. 69–84, 1971.
[6] ———, "Theories for the interaction of electromagnetic and oceanic waves: A review," *Bound. Layer Meteorol.*, vol. 13, pp. 61–85, 1978.
[7] A. Ishimaru and J. S. Chen, "Scattering from very rough surfaces based on the modified second order Kirchhoff approximation with angular and propagation shadowing," *J. Acoust. Soc. Amer.*, vol. 88, pp. 1877–1888, 1990.
[8] E. Rodriguez and Y. Kim, "A unified pertubation expansion for surface scattering," *Radio Sci.*, vol. 27, pp. 79–93, 1992.
[9] R. I. Collin, "Full wave theories for rough surface scattering: An updated assessment," *Radio Sci.*, vol. 29, pp. 1237–1254, 1994.
[10] A. G. Voronovich, "A two scale model from the point of view of the small slope approximation," *Waves Random Media*, vol. 6, p. 73, 1996.
[11] V. I. Tatarskii and S. F. Clifford, "On the theory of Δk radar observations of ocean surface waves," *IEEE Trans. Antennas Propagat.*, vol. 43, pp. 843–850, 1995.
[12] A. K. Fung, *Microwave Scattering and Emission Models and Their Applications*. Boston: Artech House, 1994.
[13] D. Holliday, G. St.-Cyr, and N. E. Woods, "A radar ocean imaging model for small to moderate incidence angles," *Int. J. Remote Sensing*, vol. 8, pp. 1323–1430, 1987.
[14] R. R. Lentz, "A numerical study of electromagnetic scattering from ocean-like surfaces," *Radio Sci.*, vol. 9, pp. 1139–1146, 1974.
[15] R. M. Axline and A. K. Fung, "Numerical computation of scattering from a perfectly conducting random surface," *IEEE Trans. Antennas Propagat.*, vol. AP-26, pp. 482–488, 1978.
[16] M. F. Chen and A. K. Fung, "A numerical study of the regions of validity of the Kirchhoff and small-perturbation rough surface scattering models," *Radio Sci.*, vol. 23, pp. 163–170, 1988.
[17] E. I. Thorsos, "The validity of the Kirchhoff approximation for rough surface scattering using a Gaussian roughness spectrum," *J. Acoust. Soc. Amer.*, vol. 83, pp. 78–92, 1988.
[18] A. K. Fung and M. F. Chen, "Numerical simulation of scattering from simple and composite random surfaces," *J. Opt. Soc. Amer. A*, vol. 2, pp. 2274–2284, 1985.
[19] C. Macaskill and B. J. Kachoyan, "Numerical evaluation of the statistics of acoustic scattering from a rough surface," *J. Acoust. Soc. Amer.*, vol. 84, pp. 1826–1835, 1988.
[20] S. L. Durden and J. F. Vesecky, "A numerical study of the separation wavenumber in the two scale scattering approximation," *IEEE Trans. Geosci. Remote Sensing*, vol. 28, pp. 271–272, 1990.
[21] E. I. Thorsos, "Acoustic scattering from Pierson–Moskowitz sea surfaces," *J. Acoust. Soc. Amer.*, vol. 88, pp. 335–349, 1990.
[22] C. L. Rino, T. L. Crystal, A. K. Koide, H. D. Ngo, and H. Guthart, "Numerical simulation of backscatter from linear and nonlinear ocean surface realizations," *Radio Sci.*, vol. 26, pp. 51–71, 1991.
[23] E. Rodriguez, Y. Kim, and S. L. Durden, "A numerical assessment of rough surface scattering theories: Horizontal polarization," *Radio Sci.*, vol. 27, pp. 497–513, 1992.
[24] Y. Kim, E. Rodriguez, and S. L. Durden, "A numerical assessment of rough surface scattering theories: vertical polarization," *Radio Sci.*, vol. 27, pp. 515–527, 1992.
[25] C. L. Rino and H. D. Ngo, "Application of beam simulation to scattering at low grazing angles: Oceanlike surfaces," *Radio Sci.*, vol. 29, pp. 1381–1391, 1994.
[26] L. Tsang, C. H. Chan, K. Pak, H. Sangani, A. Ishimaru, and P. Phu, "Monte Carlo simulations of large scale composite random rough surface scattering based on the banded matrix iterative approach," *J. Opt. Soc. Amer.*, vol. 11, pp. 691–696, 1994.
[27] L. Tsang, C. H. Chan, K. Pak, and H. Sangani, "Monte Carlo simulations of large scale problems of random rough surface scattering and applications to grazing incidence with the BMIA/canonical grid method," *IEEE Trans. Antennas Propagat.*, vol. 43, pp. 851–859, 1995.
[28] J. T. Johnson, "A note on the canonical grid method for two dimensional scattering problems," submitted for publication.
[29] K. Pak, L. Tsang, C. H. Chan, and J. T. Johnson, "Backscattering enhancement of electromagnetic waves from two dimensional perfectly conducting random rough surfaces based on Monte Carlo simulations," *J. Opt. Soc. Amer.*, vol. 12, pp. 2491–2499, 1995.
[30] J. T. Johnson, L. Tsang, R. T. Shin, K. Pak, C. H. Chan, A. Ishimaru, and Y. Kuga, "Backscattering enhancement of electromagnetic waves from two dimensional perfectly conducting random rough surfaces: A comparison of Monte Carlo simulations with experimental data," *IEEE Trans. Antennas Propagat.*, vol. 44, pp. 748–756, 1996.
[31] D. M. Milder and H. T. Sharp, "An improved formalism for rough surface scattering II: Numerical trials in three dimensions," *J. Acoust. Soc. Amer.*, vol. 91, pp. 2620–2626, 1992.
[32] D. M. Milder, H. T. Sharp, and R. A. Smith, "Numerical simulation of ultra-wideband microwave backscatter from the wind roughened sea surface," Arete Assoc., Sherman Oaks, CA, 1994, Rep. AU-94-005, .
[33] J. R. Apel, "An improved model of the ocean surface wave vector spectrum and its effects on radar backscatter," *J. Geophys. Res.*, vol. 99, pp. 16 269–16 291, 1994.
[34] L. Tsang, J. A. Kong, and R. T. Shin, *Theory of Microwave Remote Sensing*. New York: Wiley, 1985.
[35] L. B. Wetzel, "Sea clutter," ch. 13 of *Radar Handbook*, 2nd ed., M. Skolnik, Ed. New York: McGraw-Hill, 1990.
[36] G. S. Brown, "Backscattering from a Gaussian distributed perfectly conducting rough surface," *IEEE Trans. Antennas Propagat.*, vol. AP-26, pp. 472–482, 1978.
[37] L. A. Klein. and C. T. Swift, "An improved model for the dielectric constant of sea water at microwave frequencies," *IEEE Trans. Antennas Propagat.*, vol. AP-25, pp. 104–111, 1977.
[38] *Maui High Performance Computing Center World Wide Web Site*, http://www.mhpcc.edu, 1995.
[39] A. Geist, A. Beguelin, J. Dongarra, W. Jiang, R. Manchek, and V. Sunderam, "PVM 3 user's guide and reference manual," Oak Ridge Nat. Lab., Oakridge, TN, 1994, Rep. ORNL/TM-12187.
[40] G. R. Valenzuela, "Depolarization of EM waves by slightly rough surfaces," *IEEE Trans. Antennas Propagat.*, vol. AP-15, pp. 552–557, 1967.
[41] W. L. Jones, L. C. Schroeder, and J. L. Mitchell, "Aircraft measurements of the microwaves scattering signature of the ocean," *IEEE Trans. Antennas Propagat.*, vol. AP-25, pp. 52–61, 1977.

Joel T. Johnson (M'96) received the B.S. degree in electrical engineering from the Georgia Institute of Technology, Atlanta, in 1991 and the S.M. and Ph.D. degrees from the Massachusetts Institute of Technology, Cambridge, in 1993 and 1996, respectively.

He is currently an Assistant Professor with the Department of Electrical Engineering and ElectroScience Laboratory, The Ohio State University, Columbus. His research interests are in the areas of microwave remote sensing, propagation, and electromagnetic wave theory.

Dr. Johnson is a member of Tau Beta Pi, Eta Kappa Nu, and Phi Kappa Phi. He held a National Science Foundation graduate fellowship from 1991 to 1995, received the 1993 best paper award from the IEEE Geoscience and Remote Sensing Society, and has been named a 1997 Office of Naval Research Young Investigator.

Robert T. Shin (S'82–M'83–SM'90) received the B.S., MS., and Ph.D. degrees in electrical engineering in 1977, 1980, and 1984, respectively, from the Massachusetts Institute of Technology (MIT), Cambridge.

Since 1984, he has been a member of MIT Lincoln Laboratory as a Research Staff Member from 1984 to 1989, as a Senior Staff Member from 1989 to 1992, and as an Assistant Group Leader since 1992. His research interests are in the areas of electromagnetic wave scattering and propagation and theoretical model development and data interpretation for microwave remote sensing. He is a coauthor of *Theory of Microwave Remote Sensing* (New York: Wiley, 1985). Since 1987 he has served on the editorial board of the *Journal of Electromagnetic Waves and Applications* (JEWA).

Dr. Shin is a member of The Electromagnetics Academy, Americal Geophysical Union, Tau Beta Pi, Eta Kappa Nu, and Commission F of the International Union of Radio Science.

Jin Au Kong (S'65–M'69–SM'74–F'85) is a Professor of Electrical Engineering at the Massachusetts Institute of Technology, Cambridge. His research interest is in the area of electromagnetic wave theory and applications.

He has published eight books, including *Electromagnetic Wave Theory* (New York: Wiley, 1986), has more than 400 refereed articles and book chapters, and has supervised more than 120 theses. He is Editor-in-Chief of the *Journal of Electromagnetics Waves and Applications,* Chief Editor of the book series, *Progress in Electromagnetics Research,* and Editor of the Wiley Series in remote sensing.

Leung Tsang (S'73–M'75–SM'85–F'90) received the S.B., S.M., and Ph.D. degrees from the Massachusetts Institute of Technology (MIT), Cambridge, in 1971, 1973, and 1976, respectively.

He has been a Professor of Electrical Engineering at the University of Washington, Seattle, since 1986. He is coauthor of the book *Theory of Microwave Remote Sensing* (New York: Wiley, 1985). His current research interests are in remote sensing, wave propagation in random media and rough surfaces, and optoelectronics.

Dr. Tsang is a Fellow of the Optical Society of America. He was the Technical Program Chairman of the 1994 IEEE Antennas and Propagation International Symposium and was also the Technical Program Chairman of the 1995 Progress in Electromagnetics Research Symposium in Seattle. Since 1996, he has been the Editor-in-Chief of the IEEE TRANSACTIONS ON GEOSCIENCE AND REMOTE SENSING.

Kyung Pak received the B.S., M.S.E.E., and Ph.D. degrees in 1990, 1992, and 1996, respectively, from the University of Washington, Seattle.

In 1996, he joined the Radar Science and Engineering Section of the Jet Propulsion Laboratory, California Institute of Technology, Pasadena, CA. Currently, he is engaged in the studies of spaceborne scatterometer processing. His research interests include electromagnetic wave scattering from irregular and random rough surfaces, numerical simulation of wave scattering, and scatterometer processing.